NATURAL CONVECTION IN CONFINED CYLINDRICAL ENCLOSURE OF POROUS MEDIA WITH CONSTANT AND PERIODIC WALL TEMPERATURE BOUNDARY CONDITIONS

Prof.Dr. Ihsan Y. Hussain
Mech. Engr. Dept.
College of Engineering
University of Baghdad
Baghdad-Iraq.

Mohammad Mahdie Saleh
M.Sc. Student
Mech. Eng. Dept.

ABSTRACT

Numerical investigations of unsteady natural convection heat transfer through a fluid-saturated porous media in inclined cylindrical enclosure are studied by solving the governing (3-D) Darcy-Boussinesq equations using finite difference method. The momentum equation of flow was solved by Relaxation method and the energy equation by using Alternating Direction Implicit (ADI) method. The problem is analyzed for modified Rayleigh number with range of (50-300),angles of inclination (0°,25°,$45^{\circ}$$60^{\circ}$$90^{\circ}$), amplitude of sinusoidal temperature (0.2, 0.4, 0.8) and period (0.005, 0.01, 0.02). Results indicate an increase in the heat transfer with increasing of Rayleigh number, time, amplitude, angle of inclination and period. Also average and local Nusselt number were calculated and it is found that Maximum temperature and velocity occur at angle α=45 and this indicate a strong buoyancy force effect on convective flow.

الخلاصة

تم في هذا البحث، دراسة عددية لانتقال الحرارة بالحمل الطبيعي في وسط مسامي محـدد، اسـطواني ومائـل بواسـطة حـل المعادلات الثلاثية الأبعاد متضمنا (Darcy-Boussinesq equation) باستخدام طريقة الفروق المحددة. تم حل معادلة الـزخم تكراريـا بطريقة الإرخاء أما معادلة الطاقة فقد تم حلها بطريقة الاتجاه الضمني المتناوب (ADI). حللت المسألة لقيم عدد رالي (50-300) ، زوايا الميلان (0°،25°،45°،60°،90°)، الأتساع (0.2، 0.4، 0.8) والفترة (0.005، 0.01، 0.02). النتائج بينت زيادة في انتقال الحرارة مـع زيادة عدد رالي المطور، الزمن، الأتساع، زوايا الميلان والفترة. تم حساب قيمة عدد نسلت المعدل والموضعي ولقد وجد إن أعظم درجـة حرارة وأعظم قيمة للسرعة تحدث عند الزاوية (45) وهذا يعطي تنبأ عن تأثير قوي لقوة الطفو على المائع.

KEYWORD(S):Natural Convection; Cylindrical Enclosure; Porous Media; Sinusoidal Temperature Variation.

INTRODUCTION

Natural convection heat transfer in fluid-saturated porous media is a research topic of practical importance due to the many practical applications which can be modeled or approximated as transport phenomena in porous media, these flows appear in a wide variety of industrial application, as well as in many natural circumstances such as ground water flows, oil recovery processes, thermal insulation engineering, food processing, casting and welding of manufacturing processes, etc. Representative reviews of these applications and others convective heat transfer applications in porous media may be found in the resent books by

(Ingham and Pop 1998), (Nield and Bejan 1999), and **(Vafai and Hadim 2000)**, (**Mohammad and Nawaf, 2005**).Many studies were reported which deals with porous media, (**Wang and Zhang, 1990**) studied three-dimensional steady natural convection in an inclined liquid-saturated porous concentric cylinders for different variables. (**Shivakumara et.al., 2002**) studied numerically transient free convection in a vertical cylindrical annulus filled with a fluid saturated porous medium with $T_i>T_o$ while the top and bottom boundaries are adiabatic, a finite difference ADI and Successive Line Overrelaxation are used to solve the governing equations. (**Iyer and Vafai, 1999**) analyzed numerically free convection fluid flow and heat transfer in a horizontal cylindrical annulus in the presence of a porous geometric perturbation, the flow in the porous region is modeled using Brinkman-Forchheimer-Darcy model and the governing equations is modeled as (3-D) and solved numerically using Galerkin method of the finite element formulation. (**Mohammad, 2008**) studied natural convection in cylindrical enclosure of porous medium with constant and periodic wall temperature boundary conditions, the flow is modeled using Darcy model and the governing equations is solved numerically using finite difference method. Also there are studies for Cartesian enclosures such as (**Wajeeh, 2006)** who studied transient 3-D natural convection in confined porous media with periodic boundary conditions numerically and experimentally, the effect of the oscillating surface temperature on the fluid flow and heat transfer within the enclosure were determined. The purpose of the present paper is to study the natural convection flow behavior and its effects on the heat transfer and temperature distribution within a cylindrical enclosure filled with saturated porous medium and which is inclined by angle α from the horizontal, also velocity distribution and Nusselt number will be explained.

MATHEMATICAL MODEL

A schematic representation of the system under investigation is shown in **Fig.(1)**. The cylindrical system of coordinates (r,ϕ,z) is represented. The system is inclined with angle (α) from the horizontal so, the gravitational acceleration (g) acts in the negative (r,z) directions and positive (ϕ) direction as shown in **Fig.(1)**

The (3-D) cylindrical space contains a porous material of permeability (K) and porosity (ε) which is saturated with a Boussinesq fluid of viscosity (υ) and coefficient of thermal expansion (β).

From **Fig.(1)** the components of gravity can be written as follows;

$$\vec{g} = g_r i + g_\phi j + g_z k \quad (1)$$

$$\left.\begin{aligned} g_r &= -g\sin(\alpha)\cos(\phi) \\ g_\phi &= g\sin(\alpha)\sin(\phi) \\ g_z &= -g\cos(\alpha) \end{aligned}\right\} \quad (2)$$

By substituting the three components in **eqs.(1)**

$$\vec{g} = -g\sin(\alpha)\cos(\phi)i + g\sin(\alpha)\cos(\phi)j - g\cos(\alpha)k \quad (3)$$

The equations which describe the problem of natural convection in cylindrical enclosure are mass, momentum, and energy equations (**Bejan, 1984**);

C.E $$\frac{1}{r}\frac{\partial}{\partial r}(ru)+\frac{1}{r}\frac{\partial v}{\partial \phi}+\frac{\partial w}{\partial z}=0 \quad (4)$$

And from Darcy law for momentum the three components (r,ϕ,z) with the effect of gravity are as follows;

r -component

$$u=\frac{\mathrm{K}}{\mu_f}\left(-\frac{\partial p}{\partial r}+\rho_f g_r\right)= \frac{\mathrm{K}}{\mu_f}\left(-\frac{\partial p}{\partial r}-\sin(\alpha)\cos(\phi)\rho_f g\right) \quad (5)$$

ϕ -component

$$v=\frac{\mathrm{K}}{\mu_f}\left(-\frac{1}{r}\frac{\partial p}{\partial \phi}+\rho_f g_\phi\right)= \frac{\mathrm{K}}{\mu_f}\left(-\frac{1}{r}\frac{\partial p}{\partial \phi}+\sin(\alpha)\sin(\phi)\rho_f g\right) \quad (6)$$

z -component

$$w=\frac{\mathrm{K}}{\mu_f}\left(-\frac{\partial p}{\partial z}+\rho_f g_z\right)= \frac{\mathrm{K}}{\mu_f}\left(-\frac{\partial p}{\partial z}-\cos(\alpha)\rho_f g\right) \quad (7)$$

E.E

$$\left(\rho c_p\right)_m \frac{\partial \mathrm{T}}{\partial t}+\left(\rho c_p\right)_f\left[u \frac{\partial \mathrm{T}}{\partial r}+\frac{v}{r} \frac{\partial \mathrm{T}}{\partial \phi}+w \frac{\partial \mathrm{T}}{\partial \mathrm{z}}\right]=$$

$$\mathrm{K}_m^*\left(\frac{1}{r} \frac{\partial}{\partial r}\left(r \frac{\partial \mathrm{T}}{\partial r}\right)+\frac{1}{r^2} \frac{\partial^2 \mathrm{T}}{\partial \phi^2}+\frac{\partial^2 \mathrm{T}}{\partial z^2}\right) \quad (8)$$

In order to write the basic equations and variables in dimensionless form, the following factors and scales are introduced.

D: Diameter, α_m / D: velocity, $\Delta \mathrm{T}_{\circ}$: temperature, amplitude

$\frac{\left(\rho c_p\right)_m D^2}{\mathrm{K}_m^*}$: time, $\frac{\alpha_m \mu_f}{\mathrm{K}}$: pressure, $\frac{D^2}{\left(\frac{\mathrm{K}_m^*}{\left(\rho c_p\right)_m}\right)}$: period

Now we shall define the new dimensionless variables as;

$$R=\frac{r}{D}, Z=\frac{z}{D}, U=\frac{uD}{\alpha_m}, V=\frac{vD}{\alpha_m},$$

$$W=\frac{wD}{\alpha_m}, \tau=\frac{t}{\left(\rho cp\right)_m D^2 / \mathrm{K}_m^*}$$

$$\mathrm{P}=\frac{p}{\alpha_m \mu_f / \mathrm{K}}, a=\frac{\mathrm{A}}{\Delta \mathrm{T}_{\circ}}, \quad (9)$$

$$\theta=\frac{\mathrm{T}-\mathrm{T}_{\circ}}{\Delta \mathrm{T}_{\circ}}, \eta=\frac{per}{D^2 \Big/ \left(\frac{\mathrm{K}_m^*}{\left(\rho cp\right)_m}\right)}$$

The dimensionless form for the basic equations is obtained by substituting the above factors in **eqs.(4-8)** and the corresponding form of the governing equations in vector form will be as follows;

$$\nabla \cdot \vec{V}=0 \quad (10)$$

$$\vec{V}=-\nabla \vec{\mathrm{P}}+\frac{\mathrm{K}Dg}{\upsilon_f \alpha_m}\begin{bmatrix}-\sin(\alpha)\cos(\phi)\\ \sin(\alpha)\sin(\phi)\\ -\cos(\alpha)\end{bmatrix}+ \quad (11)$$

$$R_a\ \theta\begin{bmatrix}\sin(\alpha)\cos(\phi)\\ -\sin(\alpha)\sin(\phi)\\ \cos(\alpha)\end{bmatrix}$$

$$\frac{\partial \theta}{\partial \tau}+\vec{V} \cdot \nabla \theta=\nabla^2 \theta \quad (12)$$

Where: $R_a=\frac{g\beta \mathrm{K}\Delta \mathrm{T}_{\circ} D}{\upsilon_f \alpha_m}$ = Modified Raylieh number for porous medium

Since $\frac{\mathrm{K}Dg}{\upsilon_f \alpha_m}=c=$ constant so, **eqs.(11)** will be

$$\vec{V}=-\nabla \vec{\mathrm{P}}+c\begin{bmatrix}-\sin(\alpha)\cos(\phi)\\ \sin(\alpha)\sin(\phi)\\ -\cos(\alpha)\end{bmatrix}+$$

$$R_a\ \theta\begin{bmatrix}\sin(\alpha)\cos(\phi)\\ -\sin(\alpha)\sin(\phi)\\ \cos(\alpha)\end{bmatrix} \quad (13)$$

Now by introducing a vector potential (Φ) of the form

$$\vec{V}=\nabla \times \Phi \quad (14)$$

Into the formulation, the resulting equations may be solved numerically faster and more accurately. This vector potential satisfies identically the continuity equation. The potential is also solenoidal since the velocity is solenoidal (incompressible flow) (**Wajeeh, 2006**).

$$\nabla \cdot \vec{V}=\nabla \cdot(\nabla \times \Phi)=0 \quad (15)$$

So, $$\nabla \cdot \Phi=0 \quad (16)$$

$$\frac{1}{R} \frac{\partial\left(R\Phi_R\right)}{\partial R}+\frac{1}{R} \frac{\partial \Phi_\phi}{\partial \phi}+\frac{\partial \Phi_Z}{\partial Z}=0 \quad (17)$$

Taking the curl of **eqs.(13);**

$$\nabla \times \vec{V}=\nabla \times\left(-\nabla \vec{\mathrm{P}}\right)+\nabla \times(ca)+\nabla \times\left(R_a\ \theta b\right) \quad (18)$$

Where:

$$a=\begin{bmatrix}-\sin(\alpha)\cos(\phi)\\ \sin(\alpha)\sin(\phi)\\ -\cos(\alpha)\end{bmatrix}, \qquad b=\begin{bmatrix}\sin(\alpha)\cos(\phi)\\ -\sin(\alpha)\sin(\phi)\\ \cos(\alpha)\end{bmatrix}$$

And introducing **eqs.(14) and (16)** and by solving the resulting equations, this yield the following set of equations;

$$\nabla^2 \Phi_R=\left(\frac{1}{R} \frac{\partial \theta}{\partial \phi} \cos(\alpha)+\frac{\partial \theta}{\partial Z} \sin(\alpha)\sin(\phi)\right) Ra \quad (19)$$

$$\nabla^2\Phi_\phi = \left(\frac{\partial\theta}{\partial Z}\sin(\alpha)\cos(\phi) - \frac{\partial\theta}{\partial R}\cos(\alpha)\right)R_a \quad (20)$$

$$\nabla^2\Phi_Z = \left(-\frac{1}{R}\frac{\partial R\theta}{\partial R}\sin(\alpha)\sin(\phi) - \frac{1}{R}\frac{\partial\theta}{\partial\phi}\sin(\alpha)\cos\phi\right)R_a \quad (21)$$

The left hand side of the above three equations can be obtained as follows (**Hiroyuki 1981**)

$$\vec{\Omega} = \nabla\times\vec{V} = \nabla\times(\nabla\times\vec{\Phi}) = \nabla(\nabla\cdot\vec{\Phi}) - \nabla^2\Phi = -\nabla^2\vec{\Phi} \quad (22)$$

Where $\vec{\Omega}$ represents vorticity

Thus, $-\vec{\Omega} = \nabla^2\vec{\Phi}$ (23)

$$-\nabla^2\Phi_Z = \frac{\partial^2\Phi_Z}{\partial R^2} + \frac{1}{R}\frac{\partial\Phi_Z}{\partial R} + \frac{1}{R^2}\frac{\partial^2\Phi_Z}{\partial\phi^2} + \frac{\partial^2\Phi_Z}{\partial Z^2} \quad (24)$$

$$-\nabla^2\Phi_R = \frac{\partial^2\Phi_R}{\partial R^2} + \frac{1}{R^2}\frac{\partial(R\Phi_R)}{\partial R} + \frac{2}{R}\frac{\partial\Phi_R}{\partial R} + \frac{1}{R^2}\frac{\partial^2\Phi_R}{\partial\phi^2} + \frac{\partial^2\Phi_R}{\partial Z^2} + \frac{2}{R}\frac{\partial\Phi_Z}{\partial Z} \quad (25)$$

$$-\nabla^2\Phi_\phi = \frac{\partial^2\Phi_\phi}{\partial R^2} + \frac{1}{R}\frac{\partial\Phi_\phi}{\partial R} - \frac{\Phi_\phi}{R^2} + \frac{1}{R^2}\frac{\partial^2\Phi_\phi}{\partial\phi^2} + \frac{\partial^2\Phi_\phi}{\partial Z^2} + \frac{2}{R^2}\frac{\partial\Phi_R}{\partial\phi}$$

The hydrodynamic and thermal boundary conditions for the problem are;

$$\Phi_R = \Phi_Z = \frac{\partial\Phi_\phi}{\partial\phi} = 0 \quad \text{at}\ \phi = 0,\pi \quad (26)$$

$$\Phi_R = \Phi_\phi = \frac{\partial\Phi_Z}{\partial Z} = 0 \quad \text{at}\ Z = 0, L \quad (27)$$

$$\Phi_Z = \Phi_\phi = \frac{\partial(R\Phi_R)}{\partial R} = 0 \quad \text{at}\ R = R(wall) \quad (28)$$

And due to symmetry

$$\frac{\partial\Phi_R}{\partial R} = \frac{\partial\Phi_\phi}{\partial R} = \frac{\partial\Phi_Z}{\partial R} = 0 \quad \text{at R= 0} \quad (29)$$

For the temperature field, the non-dimensional thermal boundary conditions are

$$\frac{\partial\theta}{\partial\phi} = 0 \quad \text{at}\ \phi = 0,\pi \quad (30)$$

$$\frac{\partial\theta}{\partial Z} = 0 \quad \text{at}\ Z = 0, L \quad (31)$$

And due to symmetry

$$\frac{\partial\theta}{\partial R} = 0 \quad \text{at R= 0} \quad (32)$$

For the wall boundary, two cases for the cylinder temperature will be considered:

Case (1): constant wall temperature

$$\theta = 1 \quad \text{at}\ R = R(wall) \quad (33)$$

Case (2): the temperature of the side wall varies sinusoidally with time about a mean value $(\overline{\mathrm{T}}h)$ with amplitude (A) and period (per), as graphically depicted in **Fig.(2)**

$$\theta = 1 + a\sin\left(\frac{2\pi\tau}{\eta}\right) \quad \text{at}\ R = R(wall) \quad (34)$$

The initial conditions for the problem are;

Case (1): The flow is started at time $(\tau = 0)$ so,

$$\theta = U = V = W = \Phi_R = \Phi_\phi = \Phi_Z = 0 \quad everywhere \quad (35)$$

Case (2): To minimize the number of cycles that are necessary for the solution to become periodic, we began all the simulations starting from an initial temperature and flow field, and applying equation (34) with known period and amplitude we will obtain on the periodic solution (**Mohammad, 2008**).

The local and average Nusselt number for the cylinder surfaces are defined respectively as;

$$Nu = -\left.\frac{\partial\theta}{\partial R}\right|_{R=R(wall)} \quad (36)$$

$$Nu = -\frac{2D}{\pi L}\int_0^\pi\int_0^L \left.\frac{\partial\theta}{\partial R}\right|_{R=R(wall)} dZRd\phi \quad (37)$$

The components of the dimensionless velocity are related to the components of the dimensionless vector potential as follows;

$$\left.\begin{aligned} U &= \frac{1}{R}\frac{\partial\Phi_Z}{\partial\phi} - \frac{\partial\Phi_\phi}{\partial Z} \\ V &= \frac{\partial\Phi_R}{\partial Z} - \frac{\partial\Phi_Z}{\partial R} \\ W &= \frac{1}{R}\frac{\partial(R\Phi_\phi)}{\partial R} - \frac{1}{R}\frac{\partial\Phi_R}{\partial\phi} \end{aligned}\right\} \quad (38)$$

NUMERICAL FORMULATION

The above equations were approximated by finite-difference methods, the parabolic equations (energy equation) solved using the Alternating Direction Implicit (ADI) method, the Relaxation method were used for solving of elliptic equations (momentum equations).The numerical solution is obtained by dividing the domain of interest into a grid network of several nodes the position of a node on the grid is defined by the indices (i), (j), and (k) which will be used for indicating the points along (r,ϕ,z) directions respectively and the index (n) will be used for indicating the time step. A mesh of (21 x 21 x 21) grid size seamed reasonable and was be used in the present study.

Applying the (ADI) method on the energy equations yields;

i-implicit

$$a_i\theta_{i-1,j,k}^{n+1}+b_i\theta_{i,j,k}^{n+1}+c_i\theta_{i+1,j,k}^{n+1}=d_i\,f\left(\theta^n\right) \qquad (39)$$

j-implicit

$$a_j\theta_{i,j-1,k}^{n+2}+b_j\theta_{i,j,k}^{n+2}+c_j\theta_{i,j+1,k}^{n+2}=d_j\,f\left(\theta^{n+1}\right) \quad (40)$$

k-implicit

$$a_k\theta_{i,j,k-1}^{n+3}+b_k\theta_{i,j,k}^{n+3}+c_k\theta_{i,j,k+1}^{n+3}=d_k\,f\left(\theta^{n+2}\right) \quad (41)$$

Applying the Relaxation method on the momentum equations yields;

M.E. in R-component

$$\frac{\left(\theta_{i,j+1,k}-\theta_{i,j-1,k}\right)}{2R_i\Delta\phi}\cos(\alpha)Ra+\frac{\left(\theta_{i,j,k+1}-\theta_{i,j,k-1}\right)}{2\Delta Z}\sin(\alpha)\sin(\phi)Ra$$
$$+\left(\frac{\Phi_{R(i+1,j,k)}-2\Phi_{R(i,j,k)}+\Phi_{R(i-1,j,k)}}{\Delta R^2}\right)+$$
$$3\left(\frac{\Phi_{R(i+1,j,k)}-\Phi_{R(i-1,j,k)}}{R_i\Delta R}\right)+\frac{\Phi_{R(i,j,k)}}{R_i^{\,2}}$$
$$+\left(\frac{\Phi_{R(i,j+1,k)}-2\Phi_{R(i,j,k)}+\Phi_{R(i,j-1,k)}}{R_i^{\,2}\Delta\phi^2}\right)+$$
$$\left(\frac{\Phi_{R(i,j,k+1)}-2\Phi_{R(i,j,k)}+\Phi_{R(i,j,k-1)}}{\Delta Z^2}\right)$$
$$+2\left(\frac{\Phi_{Z(i,j,k+1)}-\Phi_{Z(i,j,k-1)}}{2R_i\Delta Z}\right)=Error=0$$

(42)

M.E. in ϕ-component

$$\left(\frac{\theta_{(i,j,k+1)}-\theta_{(i,j,k-1)}}{2\Delta Z}\right)\sin(\alpha)\cos(\phi)Ra$$
$$-\left(\frac{\theta_{(i+1,j,k)}-\theta_{(i-1,j,k)}}{\Delta R}\right)\cos(\alpha)Ra+$$
$$\left(\frac{\Phi_{\phi(i+1,j,k)}-2\Phi_{\phi(i,j,k)}+\Phi_{\phi(i-1,j,k)}}{\Delta R^2}\right)-\frac{\Phi_{\phi(i,j,k)}}{R_i^{\,2}}+$$
$$\left(\frac{\Phi_{\phi(i+1,j,k)}-\Phi_{\phi(i-1,j,k)}}{R_i\Delta R}\right)+\left(\frac{\Phi_{\phi(i,j+1,k)}-2\Phi_{\phi(i,j,k)}+\Phi_{\phi(i,j-1,k)}}{R_i^{\,2}\Delta\phi^2}\right)+$$
$$2\left(\frac{\Phi_{R(i,j+1,k)}-\Phi_{R(i,j-1,k)}}{2R_i^{\,2}\Delta\phi}\right)+\left(\frac{\Phi_{\phi(i,j,k+1)}-2\Phi_{\phi(i,j,k)}+\Phi_{\phi(i,j,k-1)}}{\Delta Z^2}\right)=Error=0$$

(43)

M.E. in Z-component

$$-\left(\frac{\theta_{(i,j+1,k)}-\theta_{(i,j-1,k)}}{2R_i\Delta\phi}\right)\sin(\alpha)\cos(\phi)Ra$$
$$-\left(\frac{\theta_{(i+1,j,k)}-\theta_{(i-1,j,k)}}{\Delta R}\right)\sin(\alpha)\sin(\phi)Ra\ -$$
$$\frac{\theta_{(i,j,k)}}{R_i}\sin(\alpha)\sin(\phi)Ra^*+\left(\frac{\Phi_{Z(i+1,j,k)}-2\Phi_{Z(i,j,k)}+\Phi_{Z(i-1,j,k)}}{\Delta R^2}\right)+$$
$$\left(\frac{\Phi_{Z(i,j+1,k)}-2\Phi_{Z(i,j,k)}+\Phi_{Z(i,j-1,k)}}{R_i^{\,2}\Delta\phi^2}\right)+$$
$$\left(\frac{\Phi_{Z(i,j,k+1)}-2\Phi_{Z(i,j,k)}+\Phi_{Z(i,j,k-1)}}{\Delta Z^2}\right)$$
$$+\left(\frac{\Phi_{Z(i+1,j,k)}-\Phi_{Z(i-1,j,k)}}{R_i\Delta R}\right)=Error=0$$

(44)

A computer program was developed in Fortran 90 language to perform the numerical solution. The program consists of main program and two-subroutines, in the main program, the first step is input of data then after specifying the initial and boundary conditions of the problem, the vector potential $(\Phi_R,\Phi_\phi,\Phi_Z)$ at every grid point in the domain are calculated from an iterative process, then calculate velocities (U, V, W) from $(\Phi_R,\Phi_\phi,\Phi_Z)$, after this calculate i,j,k-implicit coefficients (a, b ,c, d) for the tridiagonal systems of equations. Then calculate T at every grid point in the domain. After this the local and average Nusselt number will be calculated then printing the results in the last part of the main program. The first subroutine solves the tridiagonal system of equations formed in the calculating of the temperature field while the second subroutine calculates the average Nusselt number. The time implementation of program is between 15 to 70 minutes depending on the studied case and time intervals. The following is the numerical equations which solved by the program.

RESULTS AND DISCUSSION

Numerical results have been obtained for radius R=0.5 and length L=1, the computations were carried out for only one half of the computational domain due to symmetry about central vertical line. For the first case (constant wall temperature boundary conditions), **Figs.(3 and 4)** shows the isothermal lines and velocity vectors for different Rayleigh number and angle of inclination. It is clear that $\vec{V} = 0$ at both ends and so the velocity and temperature distributions will differ with different cross-sections. Here we choose Z=1, for temperature and 0.75 for velocity, as shown an increase in temperature and heat transfer with increase of Ra number and α and the maximum value of temperature and velocity is at α =45 since the gravity vector aligned with the flow and the density imbalance helps the circulation of the fluid inside the enclosure. The ascending and descending flows will causes the movement of convective fluid, this processes caused velocity vectors movement. **Fig.(5)** shows the variation of average Nusselt number with different Ra number and angle of inclination, it is found that as Ra number increase the Nu number increase this indicate a strong buoyancy force and more heat transferred and circulated in the enclosure. **Fig.(6)** shows the distribution of local Nusselt number and as shown the maximum value of local Nu at vertical position, its value increase with increasing Ra number and decrease with increase of (Z) due to effect of boundary layer. For the second case (periodic wall temperature boundary conditions), **Fig.(7)** shows the temperature distribution (isothermal lines) at Ra =125, Z=1, different simulations and angle of inclination (**Table 1**) show the values of amplitude and period which will be used in this study. During the first three simulations at fixed period heat transferred to enclosure is very high and increase with increasing amplitude and angle of inclination also the isothermal lines began to deform with increase of amplitude and angle, this deforming in the right side is greater than that in the left side. Hot regions formed in the height right corners and this hot regions increase with increasing amplitude, cross section, Ra, and angle of inclination. At simulation (4) a different behavior appears, the cold layer surrounding the wall, the hot layer confined in the center of enclosure, a regions of high temperature appear and began to move to right side with increase of (α ,Z). at simulations (5) also the behavior changed , the cold layer surrounding the wall, the hot layer occupies the center of cylinder, thickness of thermal boundary with increase of (Z) and decrease with increase of (α), the lines of thermal boundary becomes curvilinear with increase of (α). **Fig.(8)** shows the variation of average Nusselt number with dimensionless time, it is found that that the average Nusselt number along the hot wall varies sinusoidally according to the variation of the hot wall temperature and it increases with increase of amplitude and decrease with increase of period. The value of the Nusselt number at the hot wall fluctuates at the most, from maximum periodic value of Nu =1.7 at τ =0.0015 to a minimum value of Nu = -1.99 at τ =0.00625, this is for simulation (1), the hot wall Nusselt number is negative over a short duration of the cycle $0.0037 \geq \tau \leq 0.0087$, stating that over this time period there is an overall energy loss or a net heat transfer exiting the enclosure through the hot wall. **Fig.(9)** shows the variation of Nusselt number with time at Ra (125,200) and α=45,there is an increase in Nusselt value with increase Ra number. By comparing the average Nusselt number in this case with the case of constant wall temperature. We found in case one the average Nusselt number decreases with time until reach steady state in a curvilinear behavior and all heat is transferred to enclosure but in case two the value of average Nusselt number at hot wall is fluctuates from maximum to minimum value in a sinusoidal profile and heat is transferred to enclosure then to outside, this is the effect of period and amplitude.

A comparison was made for the case one to validate the results by convert the problem to a concentric cylinder like the study by (**Khalid, 2002**) and using his boundary conditions in the present study, choosing the Nusselt number as a comparison parameter because it gives a clear picture to heat transfer into computational domain, so, a plots gives the relation between average Nusselt number and Ra number for aspect ratio (S=1) and radius ratio (Y =2, 5, 10) are presented in **Fig.(10)** as a comparison between results of (Khalid) and present work. It is found that the same behavior of increasing in Nu number with increase of Ra is obtained, and a small difference between results is detected. Results difference is caused by difference in model, difference in grid size.

In order to describe the relation between the dependent variable (Nusselt number) and the independent variables (Raylieh number and angle

of inclination), a correlation have been made to describe the heat transfer data as in the form of ;

$$Nu=B\ (Ra^{c}.(1/(1+\cos\alpha))^{n}) \quad (45)$$

This correlation work for all range of Ra number and angles of inclination, the values of constants are;

$$Nu=0.605324899*Ra^{0.389673014}\ (1/\ (1+\cos\alpha))^{-0.07051460} \quad (46)$$

α in rad

CONCLUSIONS

Numerical results obtained for natural convection in an inclined liquid-saturated porous enclosure can be summarized as follows. Average Nusselt number increase with increase of Ra number, and increase very slightly or decrease with increase angle of inclination but in periodic case average Nusselt number increase with increase of amplitude and decrease with increase of period and increase very small with increase of Ra number and its variation is a sinusoidal profile with the time from maximum value in positive direction to a minimum in negative direction. Maximum temperature and velocity occur at α = 45and this is increase with increase Ra number. Local Nusselt number increase with increase Ra number and decrease with increase Z and maximum value of it at vertical position α = 0.

REFERENCES

- Bejan, A.; "Convective Heat Transfer", Wiley, New York, 1984.
- Hiroyuki O., and Tsutomu S., 1981"Natural Convection in Inclined Circular Cylindrical Annulus Heated and Cooled on its End Plates"**,** Int. J. Heat Mass Transfer, Vol.24, No. 4, pp.727-737.
- Iyer, S. V. and Vafai, K.; "Passive Heat Transfer Augmentation in a Cylindrical Annulus Utilizing a Porous Perturbation", Numerical Heat Transfer, Part A, 36, PP.115-128, 1999.
- Mohammad, A. A. and Saeid, N. H.; "Natural Convection in a Porous Cavity with Spatial Sidewall Temperature Variation", Int. J. of Numerical Methods for Heat and Fluid Flow, Vol.15, No.6, PP.555-566, 2005.
- Mohammad, M. S.; "Natural Convection in Confined Cylindrical Enclosure of Porous Media with Constant and Periodic Wall Temperature Boundary conditions", M.Sc. Thesis, University of Baghdad, 2008.
- Shivakumara, I. S., Prasanna, B. M. R. Rudraiah, N. and Venkatachalappa, M.; "Numerical Study of Natural Convection in a Vertical Cylindrical Annulus Using Non-Darcy Equation", J. of Porous Media, Vol.5, No.2, PP.87-102, 2002.
- Wang, B. X. and Zhang; "Natural Convection in Liquid-Saturated Porous Media between Concentric Inclined cylinder", Int. J. Heat Mass Transfer, Vol.33, PP.827-833, 1990.
- Wajeeh, K. H.; "Transient Three-Dimensional Natural Convection in Confined Porous Media with Periodic Boundary Conditions", PhD. Thesis, University of Technology, 2006.

NOMENCLATURE

Symbol	Description
a	Dimensionless amplitude
A	Amplitude
B	Constant in equation (45)
c_p	Specific heat at constant pressure
D	Diameter of cylinder
g	Acceleration due to gravity
K	Permeability
K_m^*	Effective thermal conductivity of porous media
L	Length of cylinder
Nu	Nusselt number

P	Dimensionless pressure
p	Pressure
R	Dimensionless radial coordinate
r	Radial coordinate
Ra	Raylieh number
$T_\circ$	Reference temperature
$T\bar{h}$	Mean hot wall temperature
T_h	Hot wall temperature
t	Time
U	Dimensionless component of velocity in R-direction
u	Velocity component in R-direction
V	Dimensionless component of velocity in φ -direction
v	Velocity component in φ -direction
W	Dimensionless component of velocity in Z-direction
w	Velocity component in Z-direction
Z	Dimensionless axial coordinate
z	Axial coordinate

Greek symbols	
α	Angle of inclination
α_m	Effective thermal diffusivity of porous medium
β	Volumetric thermal expansion coefficient
θ	Dimensionless temperature
ϕ	Angular coordinate
Φ	Vector potential
$\Phi_R, \Phi_\phi, \Phi_Z$	Vector potential components in R,φ and Z directions
$\rho_\circ$	Reference density at T◦
τ	Dimensionless time
per	period
η	Dimensionless period
μ	Dynamic viscosity
υ_f	Kinematic viscosity of the fluid
$\Delta R, \Delta\phi, \Delta Z$	Distance between the grid points in R,φ and Z direction
$\Delta\tau$	Interval between two time steps
∇	Del operator

Subscript	
Symbol	**Description**
f	Fluid
i, j, k	Grid points location in R,φ and Z directions
h	Hot
m	Solid
c,n	Constants in equation (45)
°	Reference

Table (1): Input Data for the Simulations

Simulation number	Ra	a	η
1	125	0.2	0.01
2	125	0.4	0.01
3	125	0.8	0.01
4	125	0.4	0.005
5	125	0.4	0.02

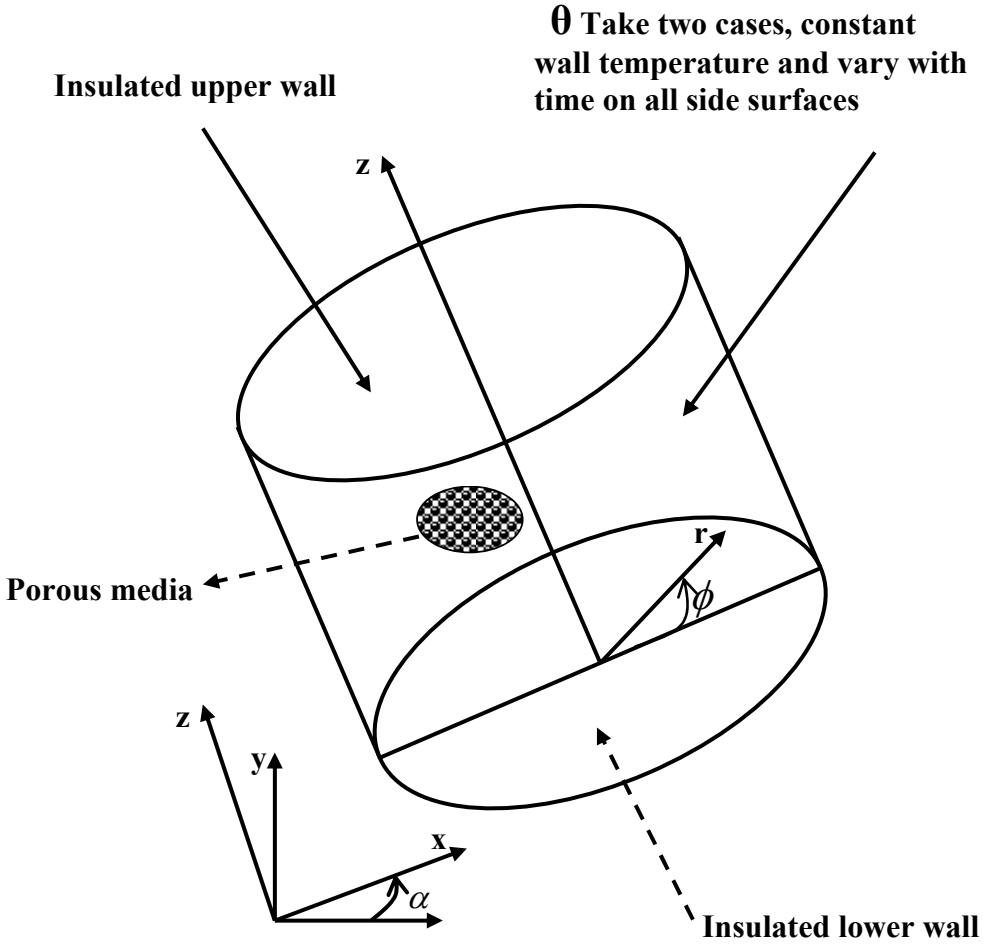

Fig.(1): Geometrical Shape of the Problem

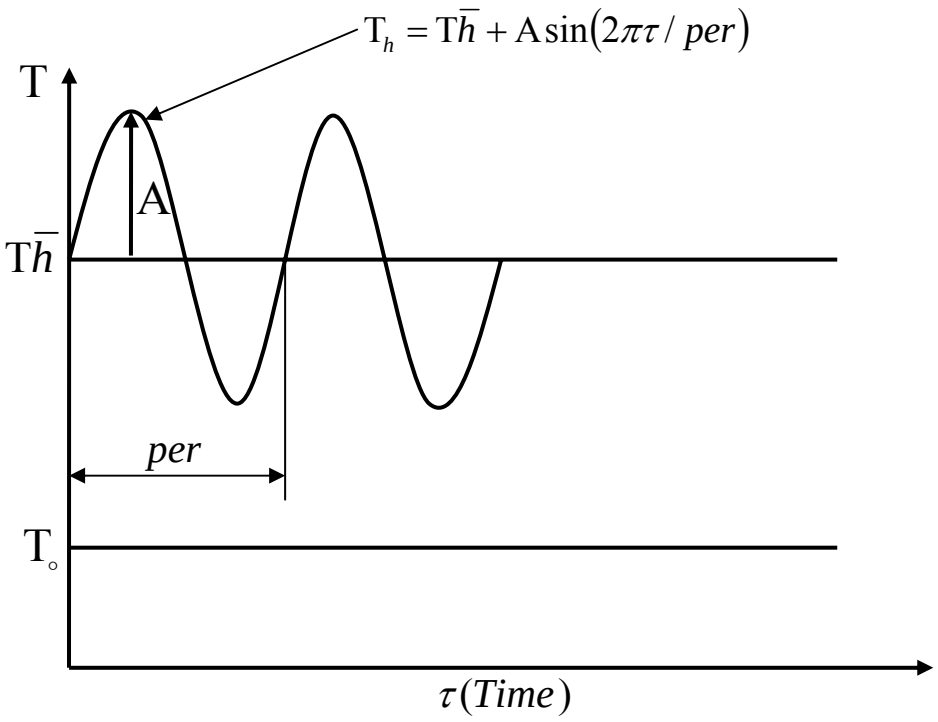

Fig.(2): The Hot Wall Time-Dependent Boundary Condition

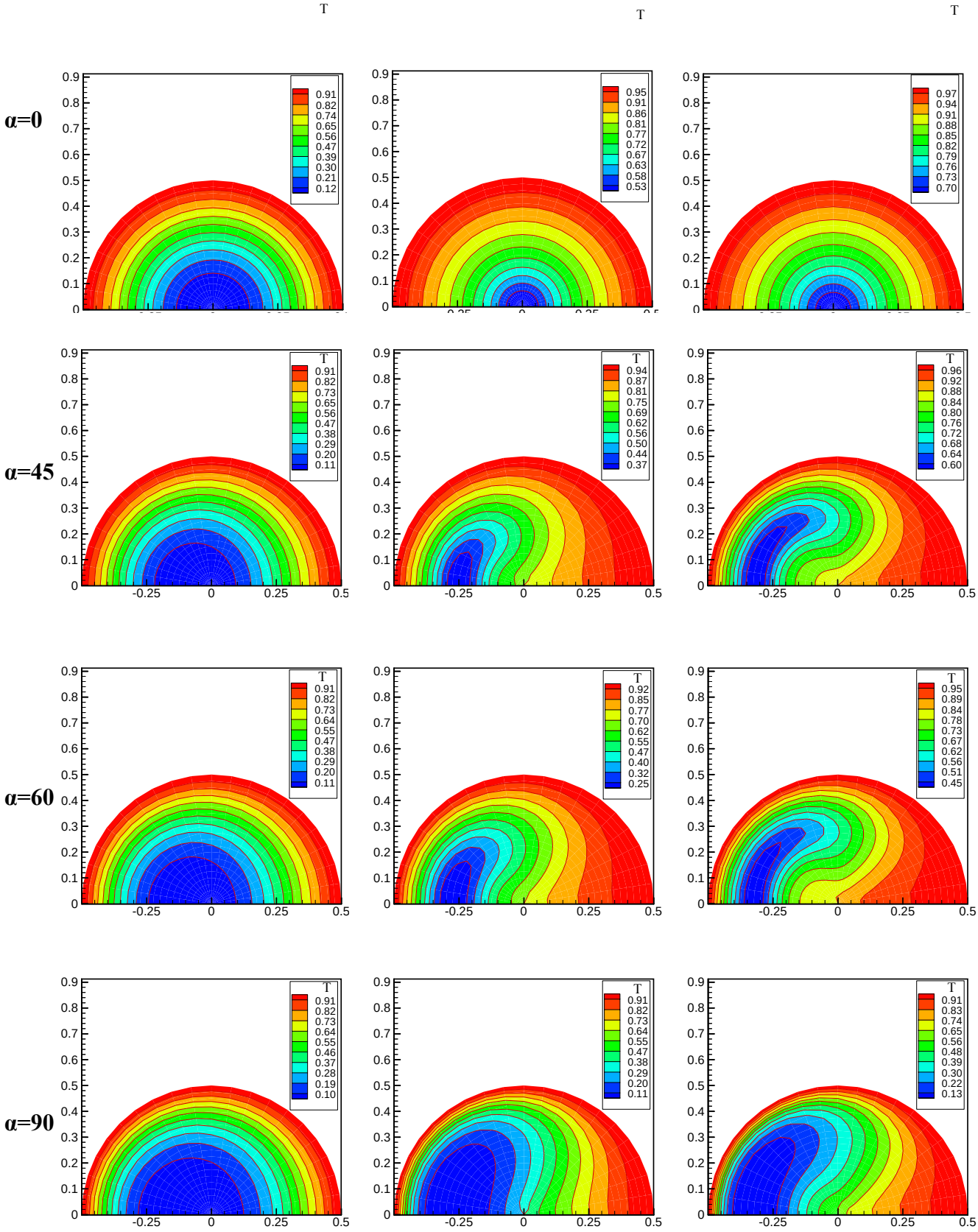

Fig.(3):Transient Temperature Distribution for Z =1

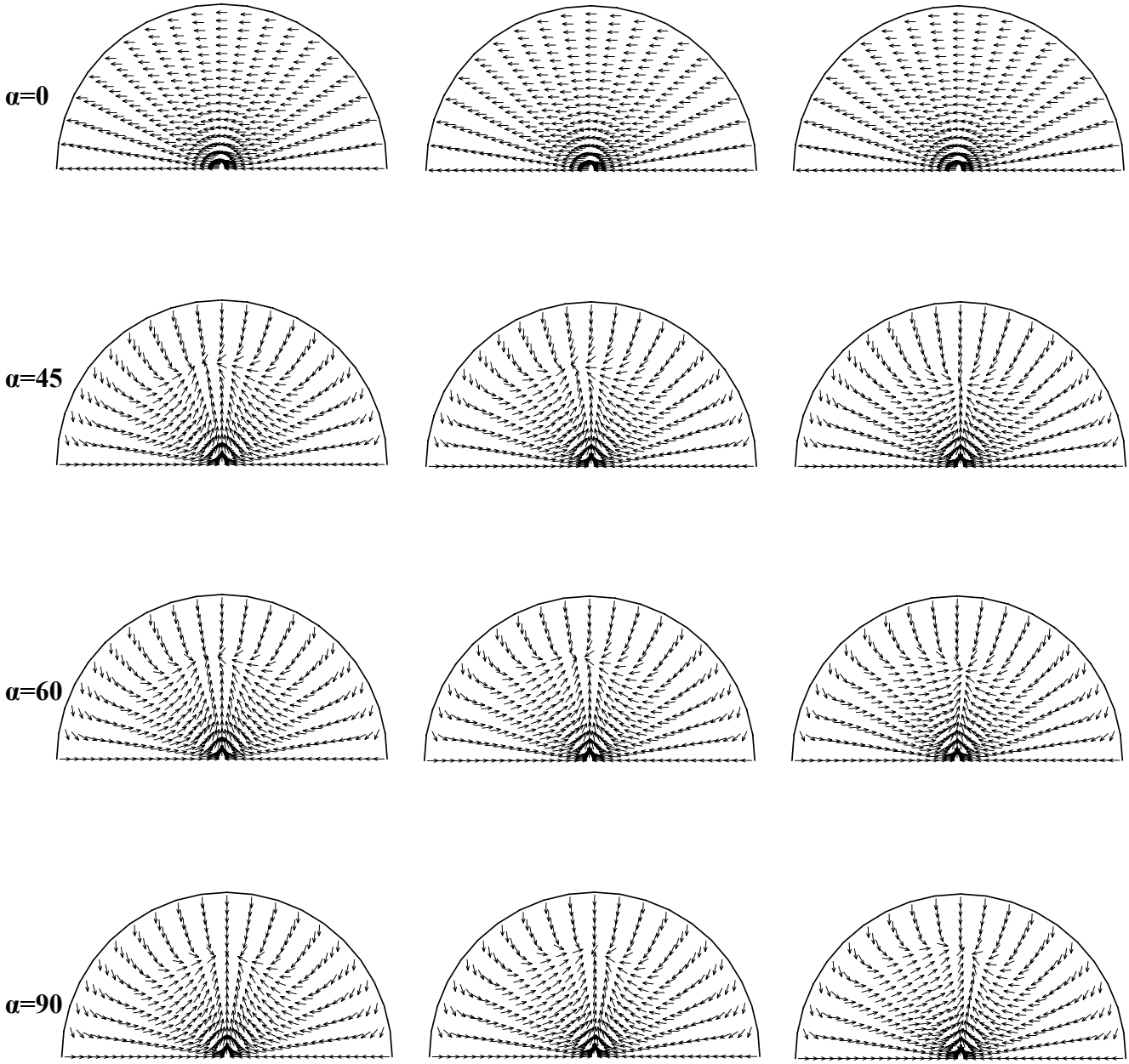

Fig.(4): Velocity vectors for Z =0.75

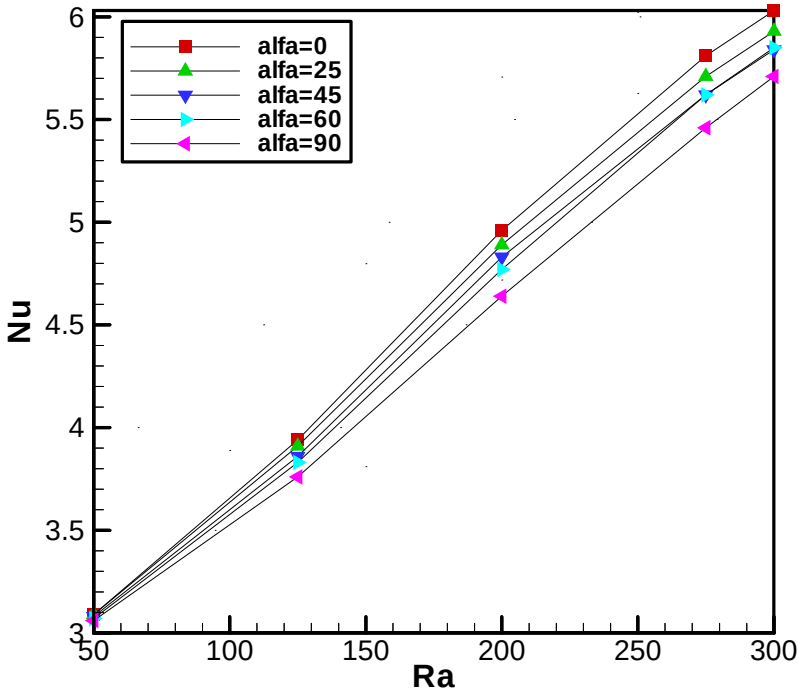

a

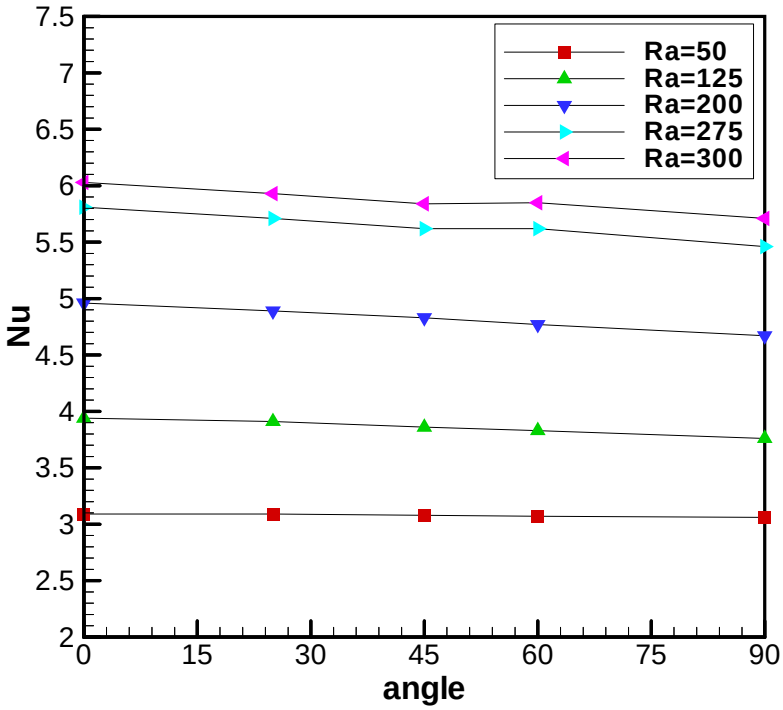

b

Fig.(5): Variation of Nusselt number, a with Ra number, b with angle of inclination

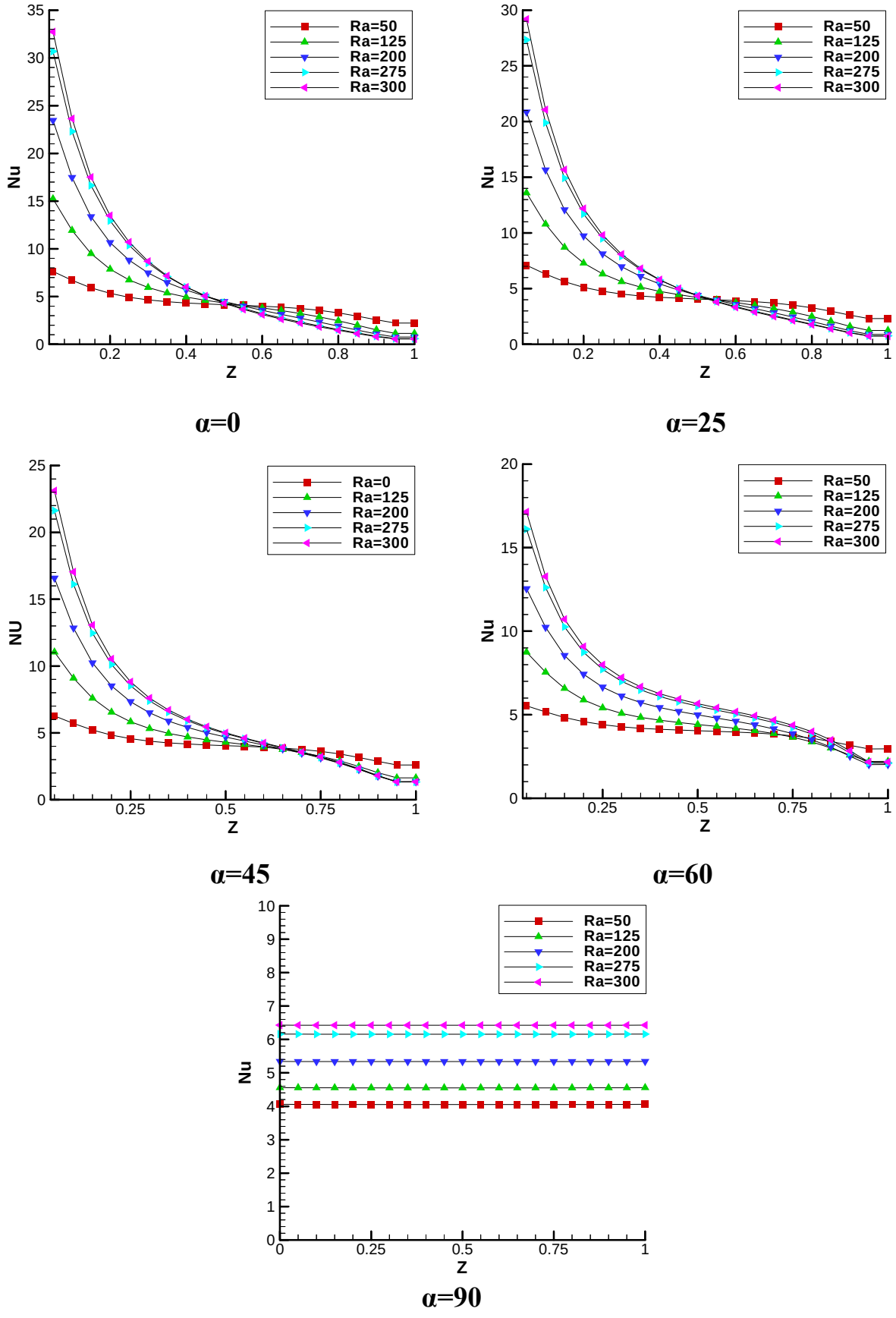

Fig.(6): Variation of Local Nusselt Number with (Z) for Different Ra Number

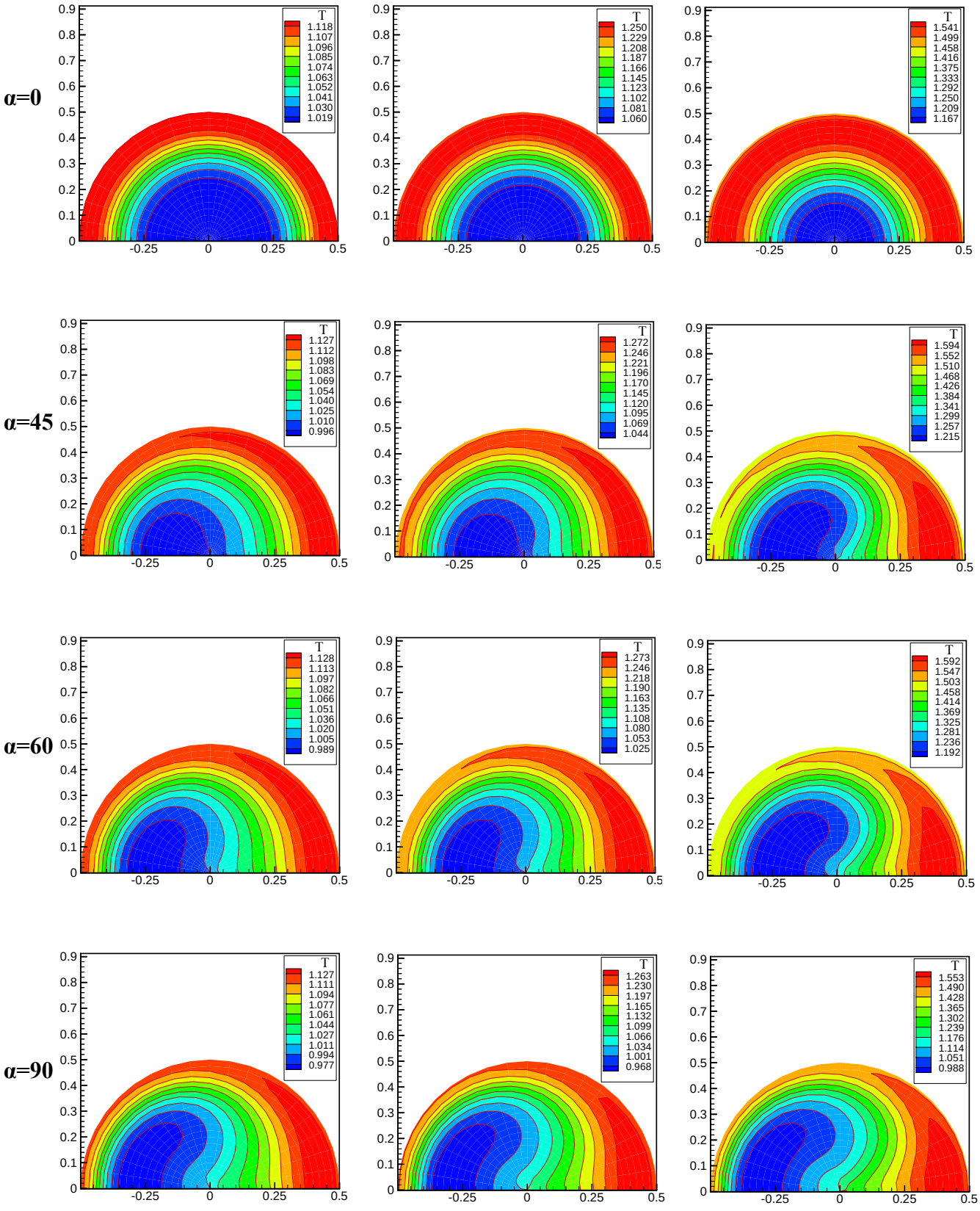

Fig.(7):Transient Temperature Distribution at Ra =125

α=0

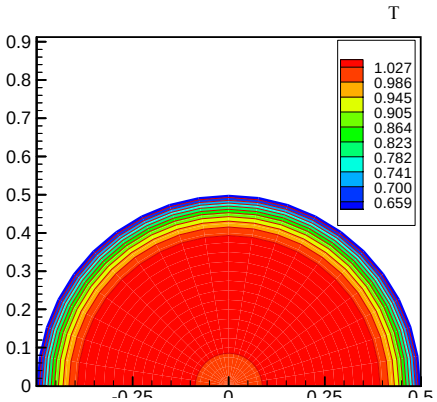

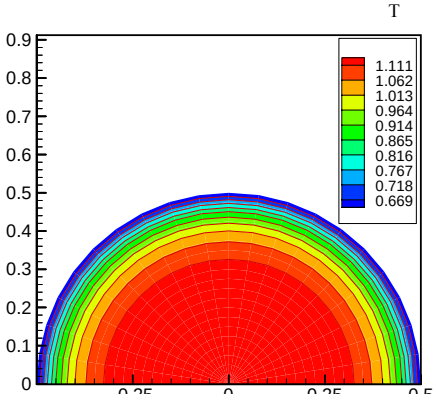

α=45

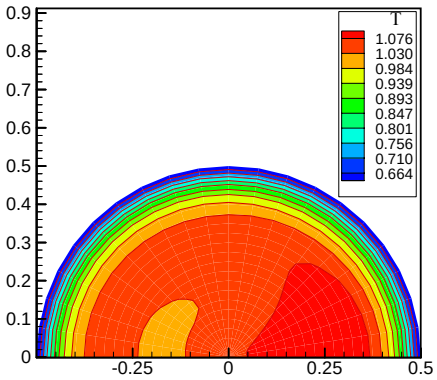

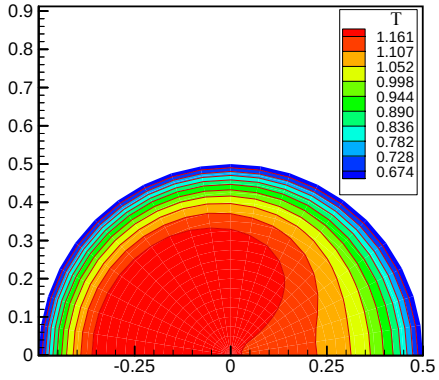

α=60

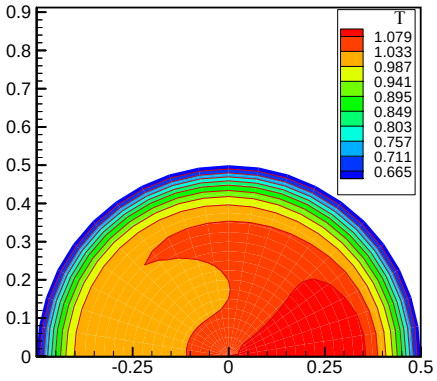

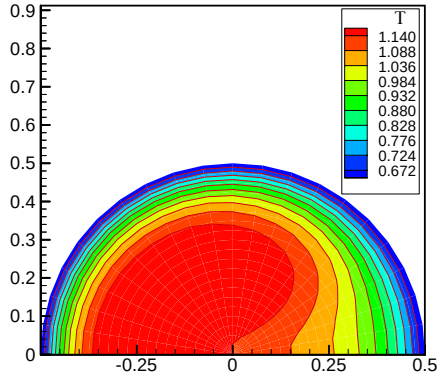

α=90

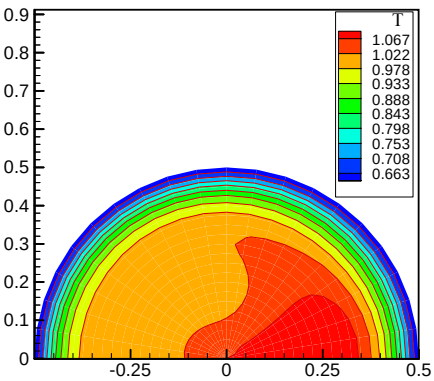

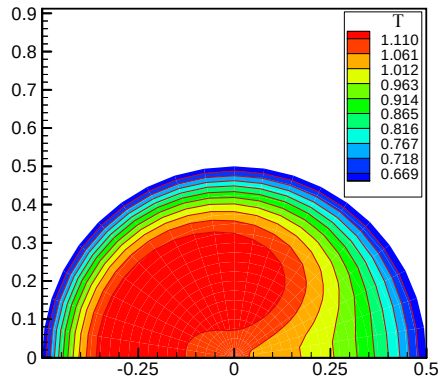

Simulation (4) **Simulation (5)**

Fig.(7): Continued

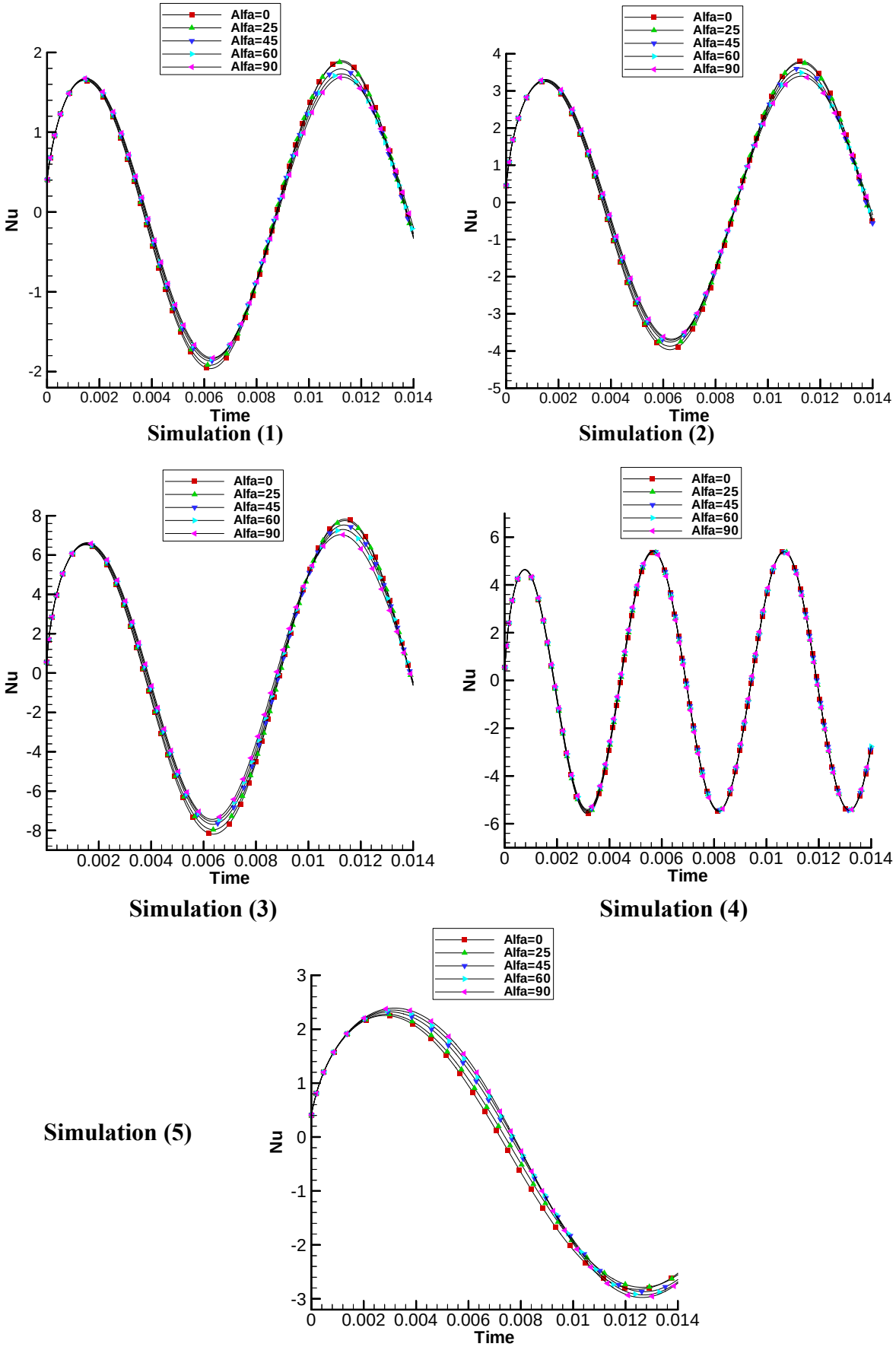

Fig.(8): Transient Nusselt Number for Different Simulations, Ra =125

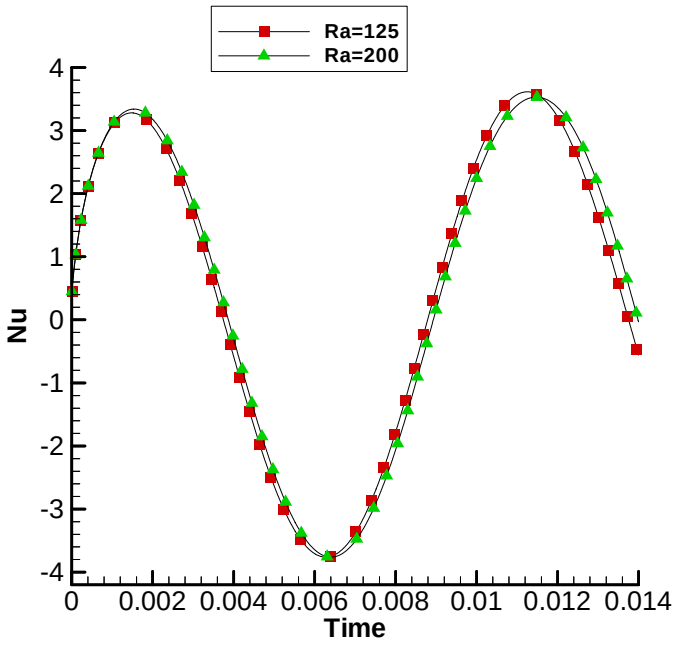

Simulation (1)

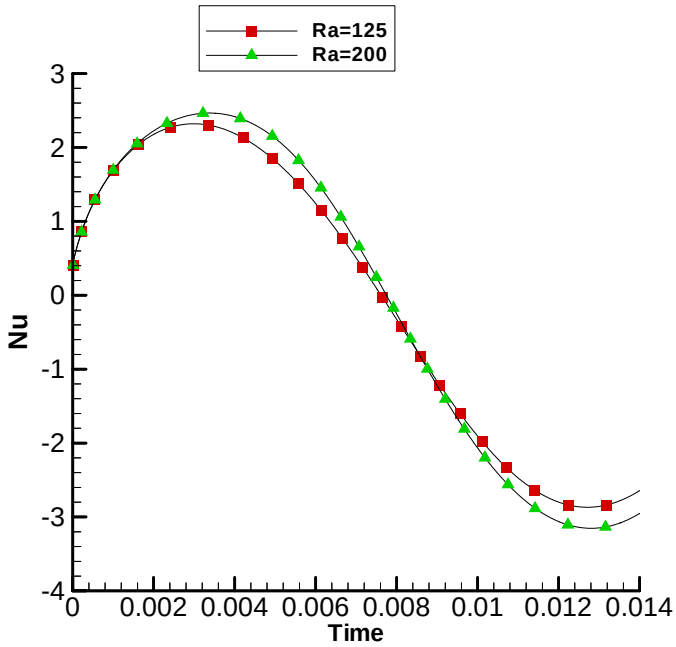

Simulation (5)

Fig.(9) Transient Nusselt Number for α =45

Y=2

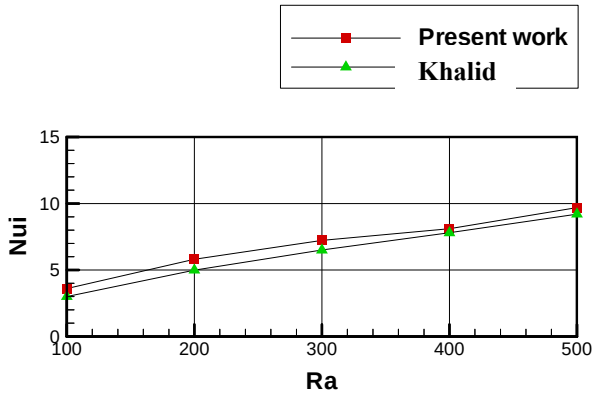

Y=5

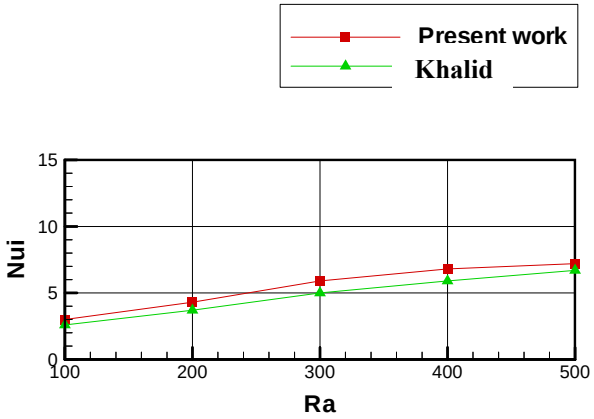

Y=10

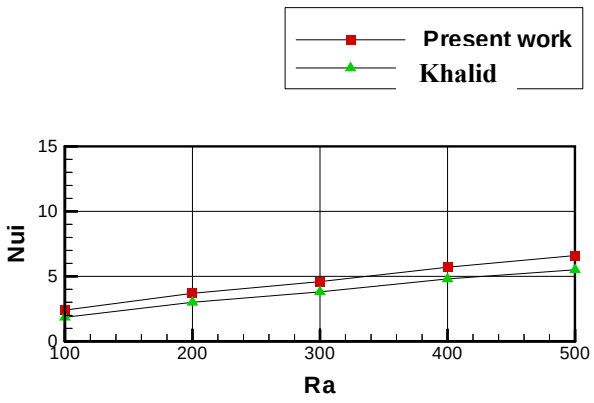

Fig.(10): Comparison of the Results